Sensors and Materials, Vol. 36, No. 2 (2024) 465–472
MYU Tokyo

S & M 3533

Dosimetric Properties of Undoped and Tb-doped $Sr_3Y(PO_4)_3$ Single Crystals

Haruaki Ezawa,* Yuma Takebuchi, Kai Okazaki, Takumi Kato, Daisuke Nakauchi, Noriaki Kawaguchi, and Takayuki Yanagida

Nara Institute of Science and Technology (NAIST), Ikoma, Nara 630-0192, Japan

(Received October 2, 2023; accepted January 18, 2024)

Keywords: dosimeter, Tb^{3+} ions, single crystal

Undoped and Tb-doped single crystals of $Sr_3Y(PO_4)_3$ were synthesized by the floating zone method, and the dosimetric properties of the obtained single crystals were investigated. The undoped crystal displayed a luminescence peak at 360 nm due to self-trapped excitons in both thermally and optically stimulated luminescence (TSL and OSL) spectra. The Tb-doped crystals showed luminescence peaks originating from 4f-4f transitions of Tb^{3+} in both TSL and OSL spectra. The 1% Tb-doped sample had the highest TSL and OSL intensities. The lower detection limits of TSL and OSL signals of the 1% Tb-doped sample were 0.01 and 0.1 mGy, respectively.

1. Introduction

Storage luminescence materials are used in imaging plates and personal and environmental monitoring.[1–5] Phosphor-type dosimetric materials are primarily divided into three categories depending on each luminescence mechanism. The first one is thermally stimulated luminescence (TSL), which occurs by the recombination of electrons and holes that are stimulated with heat and released from trapping centers.[6] The second one is optically stimulated luminescence (OSL), in which trapped electrons and holes are stimulated with light unlike TSL.[7] The third one is radio-photoluminescence (RPL), a phenomenon that creates photoluminescence (PL) centers through interactions with radiation.[8] In general, high luminescence intensity, low fading, good thermal and chemical stabilities of a host material, and wide measurable dose range are necessary for dosimetric materials. Until now, various dosimetric materials have been explored.[9–16] However, there is still a need to study novel dosimetric materials because no dosimetric materials meet all of the above requirements.

$Sr_3Y(PO_4)_3$ (SYPO) has recently attracted considerable interest as the host material of phosphors because of its large band gap, strong chemical stability, ease of adding rare-earth elements, and low synthetic sintering temperature.[17] With these attractive properties, some studies on the optical characteristics of SYPO doped with rare-earth elements have been conducted.[18–21]

*Corresponding author: e-mail: ezawa.haruaki.ec6@ms.naist.jp
https://doi.org/10.18494/SAM4757

ISSN 0914-4935
https://myukk.org/

To our best knowledge, the radiation-induced luminescence properties of SYPO have not been reported. Therefore, there is room for research into the dosimetric properties of SYPO as well as activator effects. In this investigation, undoped and Tb-doped SYPO single crystals were synthesized, and their dosimetric properties were assessed. For dosimetric materials, Tb may serve as a luminescence center. The sensitivity wavelengths of common photodetectors such as a photomultiplier tube and a Si photodiode overlap with the emission wavelengths of Tb^{3+}. Therefore, many Tb-doped dosimetric materials including Mg_2SiO_4 (TORECK, MSO-S), a commercial dosimeter, have been studied.[22–25]

2. Materials and Methods

Undoped and Tb-doped single crystals of SYPO were grown by the floating zone (FZ) method. The starting materials, namely, $SrCO_3$ (4N, Wako Pure Chemical), Y_2O_3 (4N, Furuuchi Chemical), H_6NO_4P (4N, SIGMA-ALDRICH), and Tb_4O_7 (4N, Furuuchi Chemical), were uniformly mixed. To account for the evaporation of P, 10% more H_6NO_4P was added to the stoichiometric ratio. Tb concentrations in relation to Y were 0.1, 0.5, 1, 5, and 10%. After mixing, the powders were calcined at 1100 °C for 8 h. The calcined samples were made into bars and heated at 1150 °C for 8 h. The single crystalline rod samples were synthesized using an FZ furnace (Crystal Systems Corporation, FZ-T-12000-X-VPO-PC-YH) in air atmosphere with rotation and pull-down rates of 20 rpm and 10 mm/h, respectively.

A portion of the crystals were polished using a polishing device (Buehler, MetaServ 250). For powder X-ray diffraction (XRD) measurements, another portion were ground into a powder. An X-ray diffractometer (Rigaku, MiniFlex600) with a Tl-doped NaI scintillation counter was used to measure the XRD patterns.

In the TSL measurement, the samples were irradiated with X-rays using an X-ray generator (Spellman XRB80N100/CB). With the use of a TSL reader (NanoGray Inc., TL-2000),[26] TSL glow curves were measured. The temperature range was from 50 to 490 °C, and the heating rate was 1 °C/s. An electric heater and a Si CCD-based spectrometer (Ocean Optics, QE Pro)[27] were used to investigate the TSL spectra. TSL dose response functions were computed from the highest peak height of the TSL glow curves at each irradiation dose. The irradiation dose range of X-rays was from 0.01 to 1000 mGy. For the fading property, the TSL glow curves were measured immediately or after keeping the sample for 1, 5, 24, and 48 h at room temperature.

A spectrofluorometer (JASCO, FP-8600) was used to evaluate the OSL properties. The OSL properties of the undoped sample were evaluated using an optical 510 nm shortcut filter (ASAHI SPECTRA, SCF510) and an optical 450 nm longcut filter (ASAHI SPECTRA, LCF450) to separate the stimulation and emitting photons. For the Tb-doped samples, an optical bandpass filter of 530 nm (ASAHI SPECTRA, PB0530) and an optical shortcut filter of 590 nm (ASAHI SPECTRA, SCF590) were utilized. OSL dose response functions were computed from the integrated intensity of OSL decay curves at various doses ranging from 0.01 mGy to 10 Gy. This integration time for the OSL dose response was 0–500 s. In the fading property, the OSL decay curves were measured immediately or after keeping the sample for 0.5, 1, and 2 h at room temperature.

3. Results and Discussion

Single crystalline rods of average size (5 mmφ × 20 mm) were successfully formed after the crystal growth. Since some cracks were present in the samples, portions containing relatively fewer cracks were chosen for cutting and polishing. Figure 1 shows photographs of the undoped and Tb-doped samples under room light (bottom) and 254 nm UV light (top). All the samples were clearly transparent and colorless under room light. The undoped, 0.1, 0.5, and 1% Tb-doped samples visibly exhibited no luminescence when exposed to UV light at 254 nm. The 5 and 10% Tb-doped samples displayed green fluorescence that was a typical color observed in Tb-doped phosphors.[28,29]

Figure 2 shows the XRD patterns of each sample, which closely matched the SYPO reference data (JCPDS 44-0320). In SYPO, Tb^{3+} will be replaced into Y^{3+} sites owing to their ionic radii (r) and valence.[18] No peak shifts were observed within the limits of the instrumental accuracy because the r values of Y^{3+} (coordination number (CN) = 6, r = 0.90 Å) and Tb^{3+} (CN = 6, r = 0.92 Å) are close.[30]

Figure 3 shows the TSL glow curves of the undoped and Tb-doped samples after X-ray irradiation of 10 mGy. The undoped, 0.1% Tb-doped, and other Tb-doped samples showed a glow peak at 55, 70, and 90 °C, respectively. The results indicate that Tb doping can generate new trapping centers with different energy levels. The integrated TSL intensity of the Tb-doped samples was higher in the order of the 1, 0.5, 5, 10, and 0.1% Tb-doped samples.

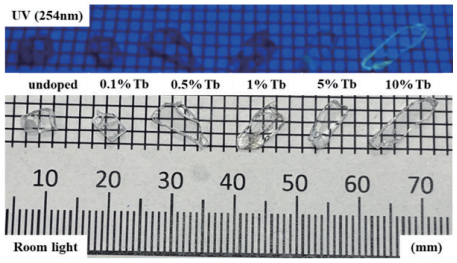

Fig. 1. (Color online) Photographs of the crystals under room light (bottom) and UV light (top).

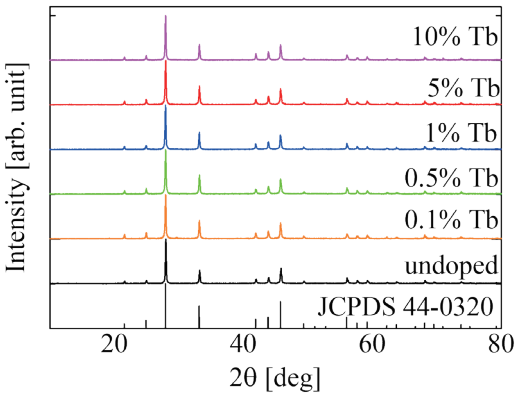

Fig. 2. (Color online) XRD patterns of the synthesized samples and reference pattern of SYPO (JCPDS 44-0320).

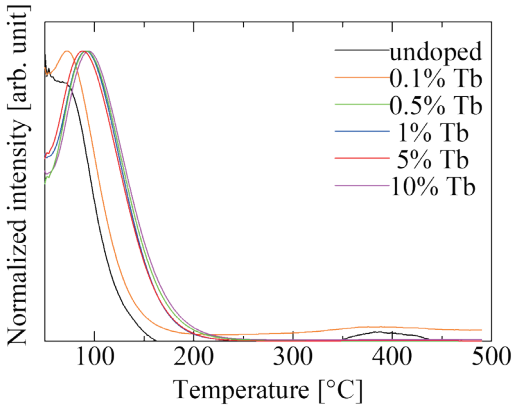

Fig. 3. (Color online) TSL glow curves of undoped and Tb-doped SYPO samples after X-ray irradiation of 10 mGy.

Figure 4 shows the TSL spectra of Tb-doped SYPO after X-ray irradiation of 10 Gy. The inset shows the TSL spectra of undoped SYPO after X-ray irradiation of 10 Gy. The undoped, 0.1% Tb-doped, and other Tb-doped samples were heated at 55, 70, and 90 °C, respectively, during measurements. In the undoped sample, two emission peaks were observed at around 360 and 600 nm. Some phosphate materials displayed similar luminescence caused by self-trapped excitons (STEs),[31–33] and the result of the undoped sample matched those of previous studies in terms of the emission wavelength at 360 nm. Therefore, the 360 nm emission peak would be ascribed to STEs. The peak at 600 nm was assumed to result from some defects. The Tb-doped samples showed emission peaks at 380, 420, 440, 460, 475, 490, 550, 590, and 620 nm, and the peaks were attributed to the 4f-4f transitions of Tb^{3+}.[34–38] Although the emission wavelengths were the same, the intensity ratios of emission lines were different, and the difference could be explained by the cross-relaxation process.[39–41]

Figure 5 shows the TSL dose response functions of the undoped and Tb-doped samples. The maximum peak height of the glow curves was used to define the intensity. The 1% Tb-doped sample showed the maximum TSL intensity among the present samples, which could be detected from 0.01 mGy. The lowest irradiation dose of the setup was 0.01 mGy, and the signal intensity when the 0.5 and 1% Tb-doped samples were exposed to 30 mGy reached the upper detection limit of the TSL reader. Therefore, these samples might be able to detect a wider dose range. Comparing the lower detection limit of those samples with those of commercial dosimeters reveals that these samples can operate at similar levels.[42] Figure 6 shows the TSL fading property of the 1% Tb-doped sample. The fading rate was estimated to be 76% for the first 24 h, and then the intensity was constant until 40 h. The fading rate was significantly higher than those of some commercial dosimeters.[43] Therefore, the samples should improve the fading properties of TSL.

Figure 7 shows the OSL spectra of Tb-doped SYPO after X-ray irradiation of 10 Gy. The inset shows the OSL spectra of undoped SYPO after X-ray irradiation of 10 Gy. An OSL peak

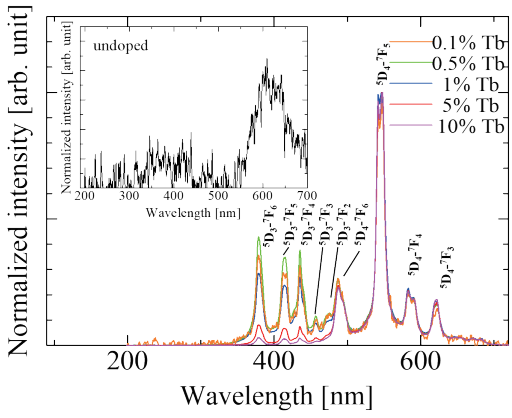

Fig. 4. (Color online) TSL spectra of Tb-doped SYPO after X-ray irradiation of 10 Gy. The inset shows TSL spectra of undoped SYPO after X-ray irradiation of 10 Gy.

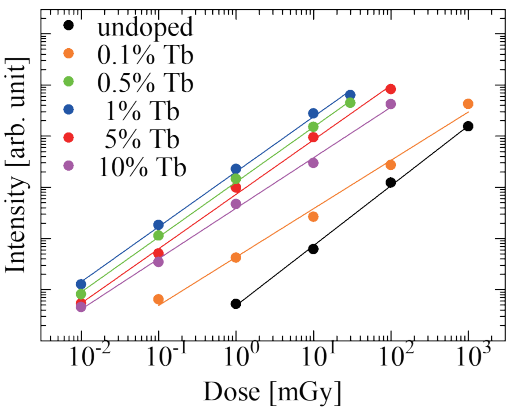

Fig. 5. (Color online) TSL dose response functions of undoped and Tb-doped samples. The tested range of irradiation dose was from 0.01 to 1000 mGy.

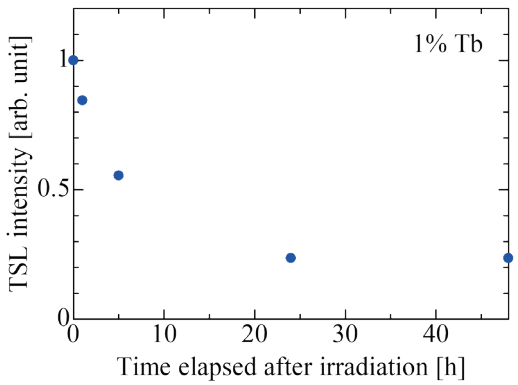

Fig. 6. (Color online) Fading property of 1% Tb-doped sample in TSL.

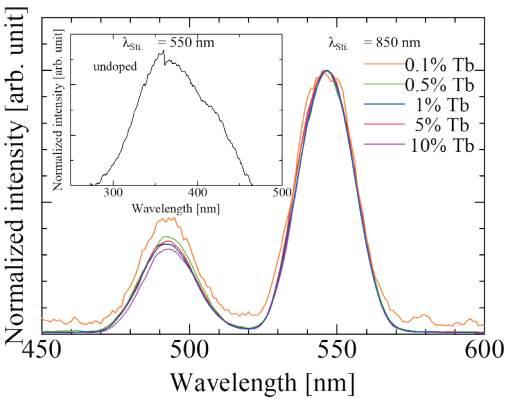

Fig. 7. (Color online) OSL spectra of Tb-doped SYPO after X-ray irradiation of 10 Gy. The stimulation wavelength for Tb-doped samples was 850 nm. The inset shows OSL spectra of undoped SYPO after X-ray irradiation of 10 Gy. The stimulation wavelength for the undoped sample was 550 nm.

was observed in the undoped sample at about 4 nm. As with TSL, this peak would be due to STE. The OSL spectra of the undoped sample were measured under stimulation from 500 to 850 nm with a 50 nm step at a monitoring wavelength of 360 nm, and the best stimulation wavelength was obtained at 550 nm. The Tb-doped samples showed two emission peaks at 490 and 550 nm. These peaks were attributed to the 4f-4f transitions of Tb^{3+}. The shapes of the TSL and OSL spectra were different since the wavelength resolution (slit width) of the OSL spectra was set to 20 nm. Therefore, the spectral shapes seemed to be broader than that of TSL. The OSL spectra of the Tb-doped samples were measured by the same method as that with the undoped one but with a monitoring wavelength of 550 nm, and the optimal stimulation wavelength of the Tb-doped ones turned out to be 850 nm. The optimal stimulation wavelengths of the undoped and Tb-doped samples were different, which indicated that Tb doping could generate new trapping centers with different energy levels. The OSL intensity of the Tb-doped samples was higher in the order of the 1, 5, 10, 0.5, and 0.1% Tb-doped samples.

Figure 8 shows the OSL dose response functions of the undoped and Tb-doped samples. The 1% Tb-doped sample produced the maximum emission intensity as well as TSL, which could be detected at 1 mGy. The measurements were carried out using standard commercial spectrofluorometers with a xenon lamp. OSL signals are typically read out by laser stimulation, which has an intensity many times higher than that of a common xenon lamp. The current findings imply that if a laser with a suitable wavelength is utilized as the stimulation source, a higher sensitivity will be attained. Figure 9 shows the fading property of the 1% Tb-doped sample in OSL. The fading rate was estimated to be 98% for 2 h. The fading rate was significantly higher than those of some commercial dosimeters also in OSL.[44,45] Hence, Tb-doped SYPO single crystals are unsuitable as OSL materials for long-period dosimetry.

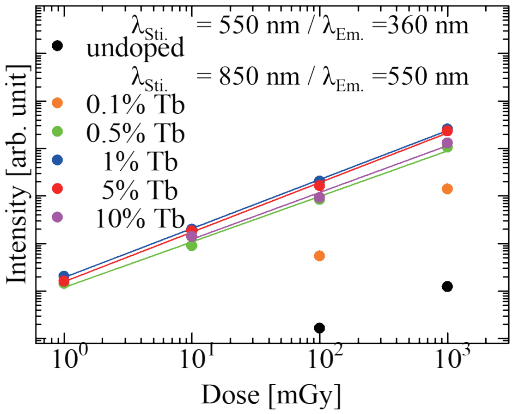

Fig. 8. (Color online) OSL dose response functions of undoped and Tb-doped samples. The stimulation and monitored wavelengths were 550 and 360 nm for the undoped sample, and 850 and 550 nm for the Tb-doped ones, respectively. The tested range of irradiation dose was from 0.01 mGy to 1 Gy.

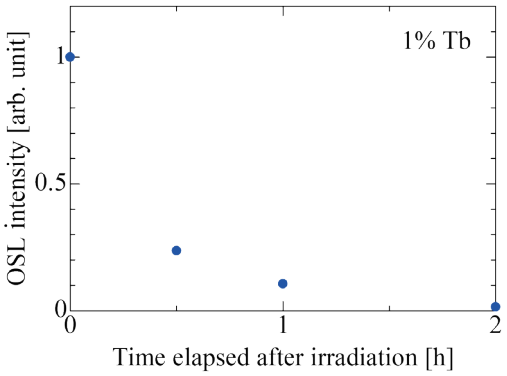

Fig. 9. (Color online) Fading property of 1% Tb-doped sample in OSL.

4. Conclusions

Undoped and Tb-doped SYPO single crystals were synthesized by the FZ method. XRD patterns revealed that all the samples were the single phase of SYPO. The undoped sample displayed luminescence ascribed by STE in both TSL and OSL. The Tb-doped samples showed luminescence due to the 4f-4f transitions of Tb^{3+} in both TSL and OSL. The highest TSL intensity was observed in the 1% Tb-doped sample, which was detectable from 0.01 mGy. The highest OSL intensity was also displayed in the 1% Tb-doped sample, which was detectable from 1 mGy. Therefore, to improve the fading properties, it is necessary to dope other dopants in future works.

Acknowledgments

This work was supported by Grants-in-Aid for Scientific Research A (22H00309), Scientific Research B (22H03872, 22H02939, 21H03733, and 21H03736), Early-Career Scientists (23K13689), and Challenging Exploratory Research (22K18997) from the Japan Society for the Promotion of Science. The Cooperative Research Project of the Research Center for Biomedical Engineering, Nippon Sheet Glass Foundation, Terumo Life Science Foundation, KRF Foundation, Tokuyama Science Foundation, Iketani Science and Technology Foundation, and Foundation for Nara Institute of Science and Technology are also acknowledged.

References

1 P. Covens, D. Berus, N. Buls, P. Clerinx, and F. Vanhavere: Radiat. Prot. Dosim. **124** (2007) 250. https://doi.org/10.1093/rpd/ncm418
2 D. Mouhssine, A. Nourreddine, A. Nachab, A. Pape, and F. Fernandez: Nucl. Instrum. Methods Phys. Res. B, **227** (2005) 609. https://doi.org/10.1016/j.nimb.2004.10.078
3 A. F. Fernandez, B. Brichard, S. O'Keeffe, C. Fitzpatrick, E. Lewis, J.-R. Vaille, L. Dusseau, D. A. Jackson, F. Ravotti, M. Glaser, and H. El-Rabii: Fusion Eng. Des. **83** (2008) 50. https://doi.org/10.1016/j.fusengdes.2007.05.034
4 T. Kato, D. Nakauchi, N. Kawaguchi, and T. Yanagida: Jpn. J. Appl. Phys. **62** (2023) 010604. https://doi.org/10.35848/1347-4065/ac94ff
5 T. Yanagida, G. Okada, and N. Kawaguchi: J. Lumin. **207** (2019) 14. https://doi.org/10.1016/j.jlumin.2018.11.004
6 K. Shinsho, R. Oh, M. Tanaka, N. Sugioka, H. Tanaka, G. Wakabayashi, T. Takata, W. Chang, S. Matsumoto, G. Okada, S. Sugawara, E. Sasaki, K. Watanabe, Y. Koba, K. Nagasaka, S. Yoshihashi, A. Uritani, and T. Negishi: Jpn. J. Appl. Phys. **62** (2023) 010502. https://doi.org/10.35848/1347-4065/ac971e
7 H. Nanto and G. Okada: Jpn. J. Appl. Phys. **62** (2023) 010505. https://doi.org/10.35848/1347-4065/ac9106
8 T. Yanagida, G. Okada, T. Kato, D. Nakauchi, and N. Kawaguchi: Radiat. Meas. **158** (2022) 106847. https://doi.org/10.1016/j.radmeas.2022.106847
9 T. Kato, D. Nakauchi, N. Kawaguchi, and T. Yanagida: Sens. Mater. **34** (2022) 653. https://doi.org/10.18494/SAM3682
10 T. Kato, H. Kimura, K. Okazaki, D. Nakauchi, N. Kawaguchi, and T. Yanagida: Sens. Mater. **35** (2023) 483. https://doi.org/10.18494/SAM4137
11 W. Chen and M. Su: Appl. Phys. Express **70** (1997) 301. https://doi.org/10.1063/1.118204
12 E. Kersting and H. von Seggern: J. Appl. Phys. **122** (2017) 084505. https://doi.org/10.1063/1.4992047
13 D. Shiratori, Y. Takebuchi, T. Kato, D. Nakauchi, N. Kawaguchi, and T. Yanagida: Sens. Mater. **34** (2022) 745. https://doi.org/10.18494/SAM3695
14 Y. Takebuchi, T. Kato, D. Nakauchi, N. Kawaguchi, and T. Yanagida: Sens. Mater. **34** (2022) 645. https://doi.org/10.18494/SAM3685
15 G. Ito, H. Kimura, D. Shiratori, D. Nakauchi, T. Kato, N. Kawaguchi, and T. Yanagida: Sens. Mater. **34** (2022) 685. https://doi.org/10.18494/SAM3681
16 H. Fukushima, D. Shiratori, D. Nakauchi, T. Kato, N. Kawaguchi, and T. Yanagida: Sens. Mater. **34** (2022) 717. https://doi.org/10.18494/SAM3691
17 F. Yang, Y. Liu, X. Tian, G. Dong, and Q. Yu: J. Solid State Chem. **225** (2015) 19. https://doi.org/10.1016/j.jssc.2014.11.025
18 Z. Leng, L. Li, X. Che, and G. Li: Mater. Des. **118** (2017) 245. https://doi.org/10.1016/j.matdes.2017.01.038
19 B. Y. Huang, B. L. Feng, L. Luo, C. L. Han, Y. T. He, and Z. R. Qiu: Mater. Sci. Eng., B **212** (2016) 71. https://doi.org/10.1016/j.mseb.2016.07.017
20 B. Yang, Z. Yang, Y. Liu, F. Lu, P. Li, Y. Yang, and X. Li: Ceram. Int. **38** (2012) 4895. https://doi.org/10.1016/j.ceramint.2012.02.080
21 A. Guan, P. Chen, L. Zhou, G. Wang, X. Zhang, and J. Tang: Spectrochim. Acta, Part A **173** (2017) 53. https://doi.org/10.1016/j.saa.2016.07.047
22 K. Ichiba, Y. Takebuchi, H. Kimura, T. Kato, D. Nakauchi, N. Kawaguchi, and T. Yanagida: Sens. Mater. **35** (2023) 475. https://doi.org/10.18494/SAM4143
23 K. Ichiba, Y. Takebuchi, H. Kimura, T. Kato, D. Nakauchi, N. Kawaguchi, and T. Yanagida: J. Mater. Sci.: Mater. Electron. **33** (2022) 13634. https://doi.org/10.1007/s10854-022-08298-3
24 H. Sakaguchi, H. Fukushima, T. Kato, D. Nakauchi, N. Kawaguchi, and T. Yanagida: J. Lumin. **254** (2023) 119533. https://doi.org/10.1016/j.jlumin.2022.119533
25 Y. Takebuchi, H. Fukushima, T. Kato, D. Nakauchi, N. Kawaguchi, and T. Yanagida: Jpn. J. Appl. Phys. **59** (2020) 052007. https://doi.org/10.35848/1347-4065/ab887c
26 T. Yanagida, Y. Fujimoto, N. Kawaguchi, and S. Yanagida: J. Ceram. Soc. Jpn. **121** (2013) 988. https://doi.org/10.2109/jcersj2.121.988
27 G. Okada, T. Kato, D. Nakauchi, K. Fukuda, and T. Yanagida: Sens. Mater. **28** (2016) 897. https://doi.org/10.18494/SAM.2016.1357
28 X. Mi, J. Sun, P. Zhou, H. Zhou, D. Song, K. Li, M. Shang, and J. Lin: J. Mater. Chem. C **3** (2015) 4471. https://doi.org/10.1039/C4TC02433H

29 W. Wang, X. Lei, Z. Ye, N. Zhao, and H. Yang: J. Alloys Compd. **705** (2017) 253. https://doi.org/10.1016/j.jallcom.2017.02.121
30 A. Guan, P. Chen, L. Zhou, G. Wang, X. Zhang, and J. Tang: Spectrochim. Acta, Part A **173** (2017) 53. https://doi.org/10.1016/j.saa.2016.07.047
31 Q. Shi, Y. Huang, K. V. Ivanovskikh, V. A. Pustovarov, L. Wang, C. Cui, and P. Huang: J. Alloys Compd. **817** (2020) 152704. https://doi.org/10.1016/j.jallcom.2019.152704
32 Y. Takebuchi, M. Koshimizu, D. Shiratori, T. Kato, D. Nakauchi, N. Kawaguchi, and T. Yanagida: Radiat. Phys. Chem. **197** (2022) 110180. https://doi.org/10.1016/j.radphyschem.2022.110180
33 Y. Takebuchi, M. Koshimizu, K. Ichiba, T. Kato, D. Nakauchi, N. Kawaguchi, and T. Yanagida: Materials **16** (2023) 4502. https://doi.org/10.3390/ma16134502
34 P. Kantuptim, T. Kato, D. Nakauchi, N. Kawaguchi, K. Watanabe, and T. Yanagida: Sens. Mater. **35** (2023) 451. https://doi.org/10.18494/SAM4141
35 R. E. Muenchausen, L. G. Jacobsohn, B. L. Bennett, E. A. McKigney, J. F. Smith, J. A. Valdez, and D. W. Cooke: J. Lumin. **126** (2007) 838. https://doi.org/10.1016/j.jlumin.2006.12.004
36 J. Hou, X. Yin, F. Huang, and W. Jiang: Mater. Res. Bull. **47** (2012) 1295. https://doi.org/10.1016/j.materresbull.2012.03.023
37 N. Kawaguchi, K. Watanabe, D. Shiratori, T. Kato, D. Nakauchi, and T. Yanagida: Sens. Mater. **35** (2023) 499. https://doi.org/10.18494/SAM4136
38 K. Ichiba, Y. Takebuchi, H. Kimura, T. Kato, D. Nakauchi, N. Kawaguchi, and T. Yanagida: Sens. Mater. **35** (2023) 475. https://doi.org/10.18494/SAM4143
39 G. X. Zhang, J. Zhang, Y. J. Liu, J. Y. Si, X. M. Tao, and G. M. Cai: J. Alloys Compd. **797** (2019) 775. https://doi.org/10.1016/j.jallcom.2019.05.059
40 B. Zhang, S. Ying, L. Han, J. Zhang, and B. Chen: RSC Adv. **8** (2018) 25378. https://doi.org/10.1039/C8RA05515G
41 A. G. Bispo-Jr, S. A. M. Lima, S. Lanfredi, F. R. Praxedes, and A. M. Pires: J. Lumin. **214** (2019) 116604. https://doi.org/10.1016/j.jlumin.2019.116604
42 V. Kortov: Radiat. Meas. **42** (2007) 576. https://doi.org/10.1016/j.radmeas.2007.02.067
43 J. A. Harvey, N. P. Haverland, and K. J. Kearfott: Appl. Radiat. Isot. **68** (2010) 1988. https://doi.org/10.1016/j.apradiso.2010.04.028
44 V. Altunal, V. Guckan, A. Ozdemir, Y. Zydhachevskyy, Y. Lawrence, Y. Yu, and Z. Yegingil: J. Lumin. **241** (2022) 118528. https://doi.org/10.1016/j.jlumin.2021.118528
45 L. Benevides, A. Romanyukha, F. Hull, M. Duffy, S. Voss, and M. Moscovitch: Radiat. Meas. **45** (2010) 523. https://doi.org/10.1016/j.radmeas.2009.12.018